Optical Cloak Design Exploiting Efficient Anisotropic Adjoint Sensitivity Analysis

L. S. Kalantari and M. H. Bakr

Department of Electrical and Computer Engineering
McMaster University, Hamilton, Ontario, L8S 4K1, Canada
kalantl@mcmaster.ca, mbakr@mail.ece.mcmaster.ca

Abstract ─ We propose in this work a novel optimization-based wideband invisibility cloaking approach at optical frequencies. We exploit the memory efficient anisotropic adjoint variable method (AVM) to significantly accelerate the sensitivity analysis with respect to the large number of parameters. Minimizing the cloaking objective function involves the gradients estimation with respect to a massive number of parameters at every iteration for time-intensive electromagnetic simulations. The AVM evaluates the required gradients over one thousand time faster than conventional methods. The significant reduction in the computational cost enables wideband optimization-based cloak design at optical region.

Index Terms ─ Adjoint variable method, computationally intensive structures, gradient-based optimization, invisibility cloaks, massive parameters, sensitivity analysis acceleration.

I. INTRODUCTION

Recently, hardware acceleration techniques and development of novel computational methods were utilized to efficiently model electrically large structures [1] – [4]. These methods enable the optimization-based design of time intensive high frequency electromagnetics structures. Several optimization techniques require estimating the gradient of an objective function with respect to all the design parameters [5]. These methods iteratively solve the optimization problem using the estimated gradients.

Some electromagnetics problems such as invisibility cloaking may have a massive number of optimizable parameters. Calculating the gradient of the objective function with respect to all those parameters may be prohibitive using conventional sensitivity analysis approaches. Gradient estimation is one of the challenges of big data analysis [6]. In conventional sensitivity analysis methods such as central finite differences (CFD), the number of required simulations to estimate the gradients scales linearly with the number of parameters. For instance, for a problem with N number of optimizable parameters, $2N$ simulations are required to find the gradient for only one iteration. This is cumbersome for huge N, particularly when the considered electromagnetic simulation is time intensive. Adjoint sensitivity analysis approaches [7] find the sensitivities with respect to all optimizable parameters regardless of their number using at most one extra simulation. Using the AVM approach, optimization-based design of electrically large structures with massive parameters, such as invisibility cloak design at optical frequencies, becomes feasible.

Invisibility cloaking have been studied through both analytical [8] – [11], scattering cancellation (SC) [8], transformation optics (TO) [9] – [11], and optimization-based [12] – [16] design approaches. Optimization methods are utilized to design multi-layered covers for structures with geometric symmetry at microwave region [12] – [15]. The resultant cloaks are usually narrowband. For wider bandwidth, the optimization process is repeated for every frequency in the band of interest [14], [15]. Optimization-based cloaking utilizes either global optimization approaches or gradient-based approaches. Global methods require too many simulations. Gradient-based methods require a possibly large number of sensitivities per iteration. This is cumbersome at optical frequencies where smaller mesh sizes make the simulations even more time intensive. These constraints limit optimization-based cloaking to narrowband structures [12], [13], [16] at microwave region [12] – [15].

Instead of following the traditional layer-based cloaks, we recently showed the strength of voxel-by-voxel cloak design in the microwave frequency regime [17], [18]. However, to solve similar problems at optical frequencies, the number of required gradients per iteration is larger than [17], [18]. Also, each simulation takes much longer time and the efficient memory usage become more critical. Thus, at optical frequencies, wideband optimization-based cloaking using classical approaches are computationally formidable.

In this work, exploiting an AVM method, we significantly accelerate the design of optical cloaks. The gradient of the cloaking objective function with respect to the massive number of parameters is estimated using

Submitted On: December 28, 2016
Accepted On: January 28, 2017

only one extra simulation. Each voxel of the cloak shell is allowed to have its independent constitutive parameters. We optimally design the generally anisotropic permittivity tensor elements of each voxel to provide sufficient invisibility for the whole structure at the two observation ports.

The manuscript is structured as follows: the formulation is presented in Section II. A wideband version of the structure studied in [11] is cloaked in Section III. We suggest a non-magnetic cloak for both transverse electric (TE) and transverse magnetic (TM) illuminations. The numerical results illustrate the efficiency of the method in wideband all-dielectrics cloak design within the optical frequency regime.

II. FORMULATION

A. Cloaking problem formulation

We aim to match the electric field of an empty domain $\boldsymbol{E}^{inc}(\boldsymbol{r},t)$ (Fig. 1 (a)), to the electric field resulting from the optimally cloaked object, $\boldsymbol{E}(\boldsymbol{r},t,\boldsymbol{p}^*)$, (Fig. 1 (b)), over the input and output spatial observation ports (Ω_{in} and Ω_{out}) and over a time domain window (T_m). Here, $\boldsymbol{r}$ is the position vector and t is time. The vector $\boldsymbol{p}$ includes all the constitutive parameters of the utilized cloak voxels. $\boldsymbol{p}^*$ is the optimal cloak constitutive parameters vector that makes $\boldsymbol{E}(\boldsymbol{r},t,\boldsymbol{p}^*)$ match $\boldsymbol{E}^{inc}(\boldsymbol{r},t)$ for all time. The following objective function measures the object invisibility:

$$F = \int_0^{T_m}\int_{\Omega_{in}} \left\| \boldsymbol{E}(\boldsymbol{r},t,\boldsymbol{p}) - \boldsymbol{E}^{inc}(\boldsymbol{r},t) \right\|_2^2 d\Omega_{in} dt + \int_0^{T_m}\int_{\Omega_{out}} \left\| \boldsymbol{E}(\boldsymbol{r},t,\boldsymbol{p}) - \boldsymbol{E}^{inc}(\boldsymbol{r},t) \right\|_2^2 d\Omega_{out} dt = \int_0^{T_m} G dt. \quad (1)$$

Here, G is the corresponding kernel of F. Ideally, if $\boldsymbol{E}(\boldsymbol{r},t,\boldsymbol{p})$ is matched to $\boldsymbol{E}^{inc}(\boldsymbol{r},t)$ over all the space and time samples, (1) would have the ideal value of zero. However, (1) can be minimized by adjusting the vector $\boldsymbol{p}$ to reach a minimum that is close to the ideal value. We utilize an all-dielectric cloak, as it provides low loss and wider band response. Such a cloak can be fabricated at optical frequencies [10], [11]. The cloak is divided into a number of voxels. Each voxel has an independent permittivity tensor, $\boldsymbol{\varepsilon}_{rj}=\text{diag}(\varepsilon_{rxxj}\ \varepsilon_{ryyj}\ \varepsilon_{rzzj})$, $j=1,2,\ldots,N_v$, where N_v is the number of cloak voxels. All tensors are non-dispersive with diagonal elements greater than one. The vector of optimizable parameters is given by:

$$\boldsymbol{p} = \left[\boldsymbol{p}_1^T \ \ \boldsymbol{p}_2^T \ \ldots \ \boldsymbol{p}_{N_v}^T \right]^T \in R^{N\times 1}. \quad (2)$$

Here, $\boldsymbol{p}_j=[\varepsilon_{rxxj}\ \varepsilon_{ryyj}\ \varepsilon_{rzzj}]^T$, $j=1,2,\ldots,N_v$ and N is the size of $\boldsymbol{p}$. To minimize (1), we utilize the steepest descent method with line search [5]. It requires estimating the gradient of (1) with respect to the N elements of $\boldsymbol{p}$ at each iteration:

$$\frac{\partial F}{\partial \boldsymbol{p}} = \left[\left(\frac{\partial F}{\partial \boldsymbol{p}_1}\right)^T \ \left(\frac{\partial F}{\partial \boldsymbol{p}_2}\right)^T \ \ldots \ \left(\frac{\partial F}{\partial \boldsymbol{p}_{Nv}}\right)^T \right]^T \in R^{N\times 1}. \quad (3)$$

As the number of cloak voxels may be large, estimating (3) using conventional CFD approaches is prohibitive.

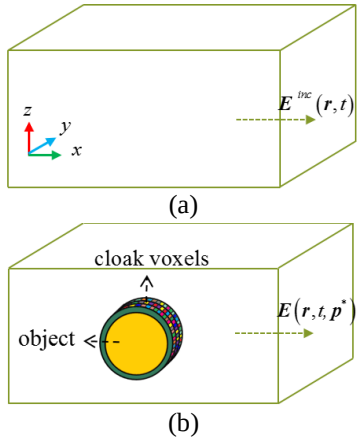

Fig. 1. The computational domain where, (a) the object is absent, and (b) a cloak shell composed of a number of optimally designed voxels covers the object.

B. AVM gradient estimation

To overcome the massive computational cost of estimating gradient vector (3), we developed a fast memory efficient anisotropic AVM algorithm. In optical frequencies, due to smaller mesh size, the number of optimizable parameters are inherently massive. Utilizing memory efficient AVM is thus mandatory as compared to [17], [18]. It estimates all gradient elements of (3) for an arbitrary wideband F, using only one extra simulation [7]. The cost of the AVM approach does not scale with the number of parameters as in classical techniques. This makes AVM well suited for applications with a relatively large number of parameters that appear in big data problems [4]. We utilize a transmission line modeling (TLM)-based AVM approach. TLM replaces the computational domain by a network of transmission lines. The electric and magnetic field components are mapped to circuit voltages and currents, v_u and i_u, $u=x,y,z$. Also, for each node of the computational domain, reflected voltages and currents, $\boldsymbol{v}^r$ and $-\boldsymbol{i}^r$, that correspond to the reflected electric and magnetic fields are defined. The total voltages and current and extra storages vectors in the original system are updated at each iteration using:

$$\begin{bmatrix} \boldsymbol{v} \\ \boldsymbol{i} \\ \boldsymbol{Q}_e \\ \boldsymbol{Q}_m \end{bmatrix} = \begin{bmatrix} 2\boldsymbol{T}_e & \boldsymbol{0} & \boldsymbol{T}_e & \boldsymbol{0} \\ \boldsymbol{0} & 0.5\boldsymbol{I} & \boldsymbol{0} & 0.25\boldsymbol{I} \\ 2\boldsymbol{I}+2\boldsymbol{\kappa}_e\boldsymbol{T}_e & \boldsymbol{0} & \boldsymbol{\kappa}_e\boldsymbol{T}_e & \boldsymbol{0} \\ \boldsymbol{0} & 4\boldsymbol{I} & \boldsymbol{0} & \boldsymbol{I} \end{bmatrix} \begin{bmatrix} \boldsymbol{v}^r \\ -\boldsymbol{i}^r \\ z^{-1}\boldsymbol{Q}_e \\ z^{-1}\boldsymbol{Q}_m \end{bmatrix}. \quad (4)$$

Here, z is the time shift operator, $\boldsymbol{\kappa}_e=\boldsymbol{\sigma}_e+8\boldsymbol{I}-4\boldsymbol{\varepsilon}_r \in R^{3\times1}$, $\boldsymbol{T}_e=(\boldsymbol{\sigma}_e+4\boldsymbol{\varepsilon}_r)^{-1}$, and $\boldsymbol{\sigma}_e$ is the electric conductivity tensor. $\boldsymbol{Q}_e$ and $\boldsymbol{Q}_m$ are the electric and magnetic extra storages vector, respectively. AVM finds the sensitivities of (1) with respect to the elements of (2), using the formula:

$$\frac{\partial F}{\partial p_i} = -\sum_j \sum_k \boldsymbol{\Lambda}_{i,j,k}^T \boldsymbol{\zeta}_{i,j,k}, \; i = 1, 2, \ldots, N. \tag{5}$$

The vectors $\boldsymbol{\zeta}_{i,j,k}=\left[\boldsymbol{\zeta}^{v^T} \quad \boldsymbol{\zeta}^{i^T} \quad \boldsymbol{\zeta}^{Q_e^T} \quad \boldsymbol{\zeta}^{Q_m^T}\right]_{i,j,k}^T \in R^{12\times1}$ represent the AVM original responses. They are evaluated during original simulation for the ith parameter, the jth cloak voxel, and the kth time-step. For all dielectric cloaks, the responses $\boldsymbol{\zeta}^i$ and $\boldsymbol{\zeta}^{Q_m}$ are zero. The responses $\boldsymbol{\zeta}^v$ and $\boldsymbol{\zeta}^{Q_e}$ are given by:

$$\boldsymbol{\zeta}^v = 2\frac{\partial \boldsymbol{T}_e}{\partial p_i}\boldsymbol{v}^r + \frac{\partial \boldsymbol{T}_e}{\partial p_i} z^{-1}\boldsymbol{Q}_e, \tag{6}$$

$$\boldsymbol{\zeta}^{Q_e} = \frac{\partial \boldsymbol{\kappa}_e}{\partial p_i}\boldsymbol{v} + \boldsymbol{\kappa}_e \boldsymbol{\zeta}^v, \tag{7}$$

the indices i, j, k are dropped for simplicity. The vectors $\boldsymbol{\Lambda}_{i,j,k}=\left[\boldsymbol{v}^{r,\Lambda^T} \quad -\boldsymbol{i}^{r,\Lambda^T} \quad \boldsymbol{B}_e^{\Lambda^T} \quad \boldsymbol{B}_m^{\Lambda^T}\right]_{i,j,k}^T \in R^{12\times1}$ are the adjoint responses. They are evaluated during adjoint simulation. $\boldsymbol{v}^{r,\Lambda}$ and $-\boldsymbol{i}^{r,\Lambda}$ are the adjoint vector of reflected field voltages and currents. $\boldsymbol{B}_e^{\Lambda}$ and $\boldsymbol{B}_m^{\Lambda}$ are the adjoint electric and magnetic extra storages. They are updated backward in time using the adjoint simulation:

$$\begin{bmatrix} \boldsymbol{v}^{\Lambda} \\ \boldsymbol{i}^{\Lambda} \\ \boldsymbol{B}_e^{\Lambda} \\ \boldsymbol{B}_m^{\Lambda} \end{bmatrix} = \begin{bmatrix} 2\boldsymbol{T}_e^T & \boldsymbol{0} & (2\boldsymbol{I}+2\boldsymbol{\kappa}_e\boldsymbol{T}_e)^T & \boldsymbol{0} \\ \boldsymbol{0} & 0.5\boldsymbol{I} & \boldsymbol{0} & 4\boldsymbol{I} \\ \boldsymbol{T}_e^T & \boldsymbol{0} & (\boldsymbol{\kappa}_e\boldsymbol{T}_e)^T & \boldsymbol{0} \\ \boldsymbol{0} & 0.25\boldsymbol{I} & \boldsymbol{0} & \boldsymbol{I} \end{bmatrix} \begin{bmatrix} \boldsymbol{v}^{r,\Lambda} \\ -\boldsymbol{i}^{r,\Lambda} \\ z\boldsymbol{B}_e^{\Lambda} \\ z\boldsymbol{B}_m^{\Lambda} \end{bmatrix}. \tag{8}$$

In the adjoint simulation the vector of nodal excitation depend on the objective function [7]. In our cloaking problem G in (1), is composed of 2 surface integrals over Ω_{in} and Ω_{out}. Thus, in the adjoint simulation, 2 excitation ports, located at Ω_{in} and Ω_{out}, are applied. This is in contrast to the case of [17], [18] where the objective function matches the electric fields at one observation plane only.

C. Possible fabrication

The effective medium theory (EMT) and alternating layered structures [10], [11] have been applied to fabricate all dielectric cloaks at optical frequencies. Mixing different dielectrics with proper filling factors produce anisotropic materials with desired anisotropy tensor. For instance, consider a composite that is made of dielectrics ε_1 and ε_2 with filling factors f_1 and f_2. The EMT formula is [11]:

$$f_1\frac{\varepsilon_1-\varepsilon_{eff}}{\varepsilon_1+\kappa\varepsilon_{eff}} + f_2\frac{\varepsilon_2-\varepsilon_{eff}}{\varepsilon_2+\kappa\varepsilon_{eff}} = 0, \tag{9}$$

where ε_{eff} is the isotropic effective permittivity and κ is the screening factor [11]. The desired anisotropic permittivity tensor can be written as [10]:

$$\begin{bmatrix} \varepsilon_{\parallel} & 0 \\ 0 & \varepsilon_{\perp} \end{bmatrix}, \; \varepsilon_{\parallel} = f_1\varepsilon_1 + f_2\varepsilon_2, \; \varepsilon_{\perp} = \frac{\varepsilon_1\varepsilon_2}{f_2\varepsilon_1 + f_1\varepsilon_2}. \tag{10}$$

Here, index $\parallel$ and $\perp$ show the cases with the electric field polarized parallel and perpendicular to the interfaces of the ε_1 and ε_2 layers. Thus, by properly selecting the dielectrics components, changing the filling factors and orientation of the composite components, the desired cloak parameters are generated using (9) and (10).

III. NUMERICAL EXAMPLE

We design a wideband dielectric cloak for the example presented in [11] for both the TE and TM illuminations. The cloaked object is a copper cylinder with a radius $R_0=21.5\Delta l$ and electric conductivity $\sigma_e=5.6\times10^7$ Sm^{-1}. The object is placed at the center of a waveguide with dimension $d_1\times d_2$, where $d_1=758\Delta l$ and $d_2=380\Delta l$ (see Fig. 2). $\Delta l=21.09$ nm is the TLM space step [7]. The object invisibility is measured by (1), where Ω_{in} and Ω_{out}, are located at $5\Delta l$ and $750\Delta l$ from the starting edge of the waveguide in x direction. For x and y boundaries, 70 layers of a perfectly matched layer are utilized. The excitation is a wideband Gaussian modulated sinusoidal (wavelength 632.8 nm and 127 nm bandwidth). The simulations are conducted on an Intel®Xeon® CPU×5670 @ 2.93 GHz (48.0 GB of RAM).

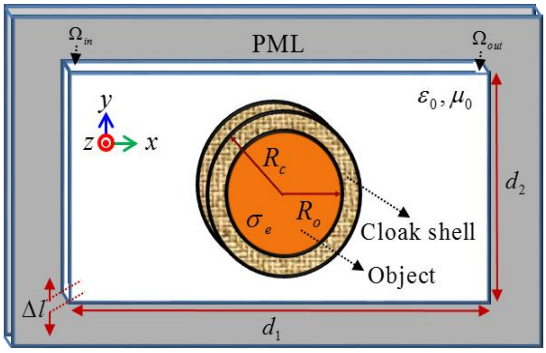

Fig. 2. The copper cylinder is covered by a cloak shell composed of a number of voxels.

A. TE illumination

We cover the object with a shell of thickness $5\Delta l$ ($R_c=26.5\Delta l$ in Fig. 2). The shell is composed of 1320 voxels. To force TE illumination, E_z (electric field polarized along z-axis) incident field is applied combined with electric wall in z boundaries. Here, E_z is the only electric field in the domain and (1) is only sensitive to ε_{rzzj}, $j=1,2,\ldots,1320$. The vector $\boldsymbol{p}$ has thus 1320 elements, ε_{rzzj}. Setting $\varepsilon_{rxxj}=\varepsilon_{ryyj}=\varepsilon_{rzzj}$, the cloak uses dielectric materials with isotropic permittivities greater than 1.

To minimize (1), the gradient vector (3), which is composed of 1320 components is estimated per iteration. The AVM calculates (3) using only 2 simulations in 118 minutes. The CFD requires 2640 simulations where each simulation takes 50.5 minutes. Therefore, in total it takes 92.5 days to estimate (3) for only one iteration using CFD! For this example at each iteration, AVM is 1129 times faster than CFD. Thus, minimizing (1) without AVM is simply prohibitive because of the large number of parameters and the intensive simulation time.

For the bare and cloaked object, the F has the values 1843 and 273 [$V^2m^{-2}s$], respectively. Figure 3 (a) illustrates the reduction of (1) per iteration. The optimal cloak parameters are within the range $1< \varepsilon_{rzzj} <18$, $\forall j$. Their distributions are presented in Fig. 3 (b). The snapshots of time-dependent E_z distributions throughout the waveguide, at the same time sample, for the bare object, empty space, and clocked object are shown in Figs. 4 (a), (b), and (c), respectively. Applying the optimally designed cloak matches the E_z distribution of the cloaked object (Fig. 4 (c)) to that of the empty space (Fig. 4 (b)) at Ω_{in} and Ω_{out}. Also, for the bare object (Fig. 4 (a)), field distortions are observed at both Ω_{in} and Ω_{out}. However, those distortions have been significantly reduced for the cloaked cylinder (Fig. 4 (c)).

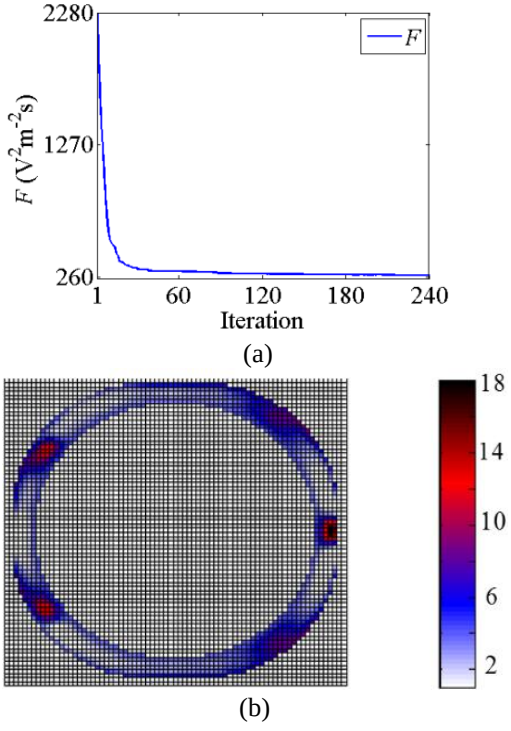

Fig. 3. TE illumination: (a) objective function per iteration, and (b) the distributions of ε_{rzzj} of the cloak voxels.

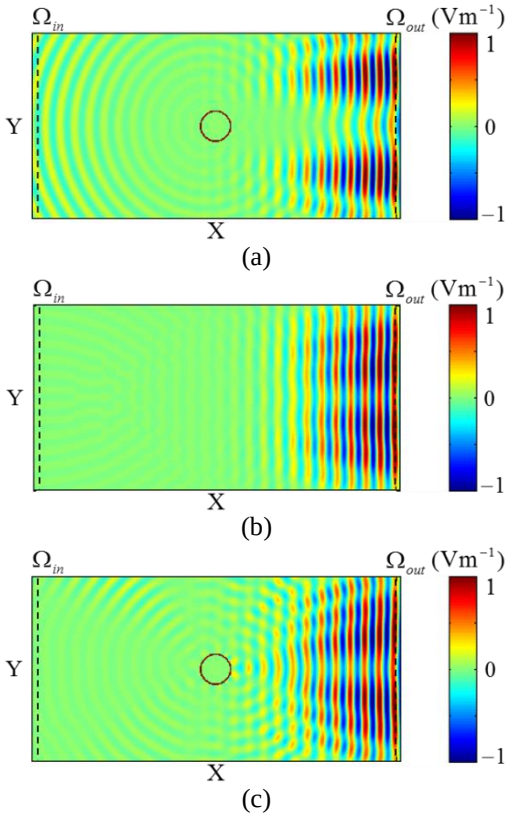

Fig. 4. TE illumination; the snapshots of E_z distributions throughout the waveguide for the: (a) bare object, (b) empty waveguide, and (c) cloaked object. Dashed lines locate Ω_{in} and Ω_{out}.

B. TM illumination

Here, the object is covered by a shell with thickness $3\Delta l$ (R_c=24.5Δl) which is composed of 768 voxels. To provide TM illumination, an incident magnetic field H_z (polarized along z-axis) is applied combined with magnetic wall boundary condition in z-direction. The electric fields in the domain are E_x and E_y. Applying the optimally designed cloak matches the E_x and E_y distributions of the cloaked object to that of the empty space. Therefore, (1) is only sensitive to ε_{rxxj} and ε_{ryyj} for j=1, 2,…,768. For simplicity, ε_{rzzj} are set equal to any of ε_{rxxj} or ε_{ryyj}. The vector $\boldsymbol{p}$ has 1536 parameters comprised of ε_{rxxj} and ε_{ryyj}, $\forall j$. Finally, the anisotropic cloak material is simplified to uniaxial crystals with diagonal tensor elements greater than one. In optimization process, the gradient vector (3), with 1536 components, is calculated per iteration. AVM approximate all those gradients by running only 2 simulations in 107 minutes. CFD would require 3072 simulations where each simulation takes 50.4 minutes. In total, using CFD, estimation of (3) takes 107.5 days per iteration! For this example AVM is 1449

times faster than CFD. Thus, minimizing (1) without AVM is simply not possible, due to the massive computation cost.

For the bare and cloaked object, F is 403.7 and 51.7 [$V^2m^{-2}s$], respectively. The optimal cloak parameters are within the range $1< \varepsilon_{rxxj} <18.2$ and $1< \varepsilon_{ryyj} <19.2$, $\forall j$. Figures 5 (a) and (b) show the optimal ε_{rxxj} and ε_{ryyj} distributions of the cloak voxels. Figure 5 (c) illustrates the reduction of (1) per iteration. Snapshots of the time-dependent H_z distributions throughout the waveguide for the bare object, empty space, and cloaked object, at a same time sample, are shown in Figs. 6 (a), (b), and (c), respectively. It illustrates that the cloaked object H_z distribution (Fig. 6 (c)) is well matched to that of the empty space (Fig. 6 (b)) at Ω_{in} and Ω_{out}. Also, the field distortions at Ω_{in} and Ω_{out} are reduced for the cloaked object (Fig. 6 (c)) as compared to the bare object (Fig. 6 (a)).

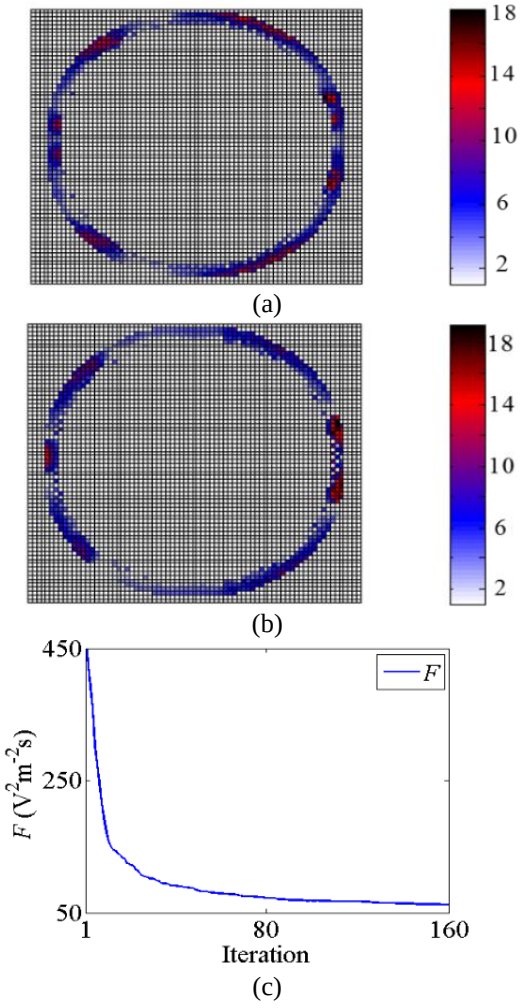

Fig. 5. TM illumination; the distributions of the optimal: (a) ε_{rxxj} and (b) ε_{ryyj} of the cloak voxels. (c) Objective function per iteration.

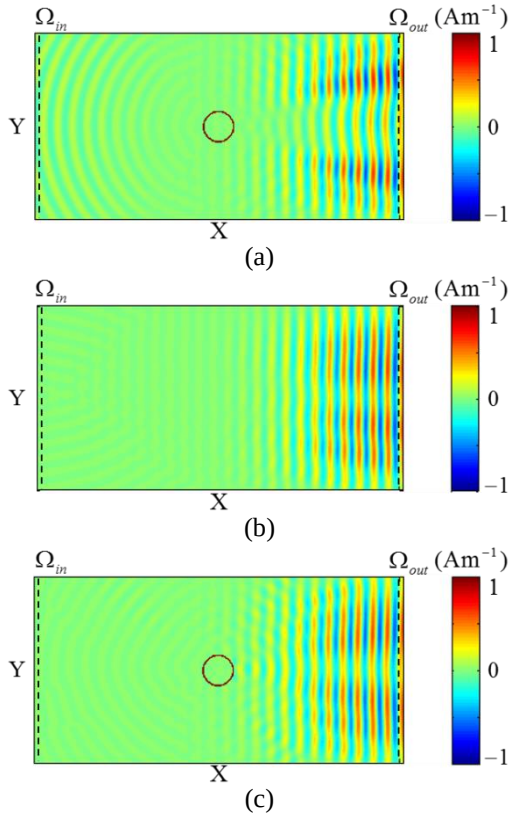

Fig. 6. TM illumination; the snapshots of the H_z distributions throughout the waveguide for the: (a) bare object, (b) empty space, and (c) cloaked object.

IV. CONCLUSION

Exploiting a fast anisotropic memory efficient AVM simulator, an all-dielectric wideband cloaks are designed at optical frequency region for both TE and TM illuminations. Designing such cloaks using classical approaches is prohibitive at optical frequencies due to the formidable computation cost. The sensitivities of a cost function with respect to a huge number of parameters are required per iteration. Our anisotropic AVM simulator significantly accelerates the sensitivities computation cost enables wideband invisibility cloaking at optical frequencies.

REFERENCES

[1] W. Yu, X. Yang, Y. Liu, R. Mittra, D. Chang, C. Liao, M. Akira, W. Li, and L. Zhao, "New development of parallel conformal FDTD method in computational electromagnetics engineering," *IEEE Antennas and Propag. Magzine*, vol. 53, pp. 15-41, 2011.

[2] W. Yu, X. Yang, Y. Liu, R. Mittra, Q. Rao, and A. Muto, "High performance conformal FDTD techniques," *IEEE Microwave Magazine*, vol. 11, pp. 42-55, 2010.

[3] W. Yu, W. Li, A. Elsherbeni, and Y. R. Samii, *Advanced Computational Electromagnetic Methods and Applications*. Norwood, MA: Artech House, 2015.
[4] E. Haber, *Computational Methods in Geophysical Electromagnetics*. Philadelphia, PA: Society for Inducterial and Applied Mathematics, 2015.
[5] M. H. Bakr, *Nonlinear Optimization in Electrical Engineering with Applications in Matlab©*. London, UK: IET, 2013.
[6] J. Fan, F. Han, and H. Liu, "Challenges of big data analysis," *Natl. Sci. Rev.*, vol. 1, pp. 293-314, 2014.
[7] L. S. Kalantari, O. S. Ahmed, M. H. Bakr, and N. Nikolova, "Adjoint sensitivity analysis of 3D problems with anisotropic materials," *IEEE Int. Microw. Symp. Digest*., Tampa Bay, FL, pp. 1-3, 2014.
[8] A. Alù and N. Engheta, "Achieving transparency with plasmonic and metamaterial coatings," *Phys. Rev. E*, vol. 72, pp. 016623, 2005.
[9] J. B. Pendry, D. Schurig, and D. R. Smith, "Controlling electromagnetic fields," *Science*, vol. 312, no. 5781, pp. 1780-1782, 2006.
[10] J. Zhang, L. Liu, Y. Luo, S. Zhang, and N. A. Mortensen, "Homogeneous optical cloak constructed with uniform layered structures," *Opt. Express*, vol. 19, no. 9, pp. 8625-8631, 2011.
[11] W. Cai, U. K. Chettiar, A. V. Kildishev, and V. M. Shalaev, "Optical cloaking with metamaterials," *Nat. Photon*., vol. 1, pp. 224-227, 2007.
[12] B. I. Popa and S. A. Cummer, "Cloaking with optimized homogeneous anisotropic layers," *Phys. Rev. A*., vol. 79, pp. 023806, 2009.
[13] J. Andkjaer and O. Sigmund, "Topology optimized low-contrast all-dielecteric optical cloak," *Appl. Phys. Lett*., vol. 98, pp. 021112, 2011.
[14] X. Wang and E. Semouchkina, "A route for efficient non-resonance cloaking by using multilayer dielectric coating," *Appl. Phys. Lett*., vol. 102, pp. 113506, 2013.
[15] Y. Urzhumov, N. Landy, T. Driscoll, D. Basov, and D. R. Smith, "Thin low-loss dielectric coatings for free-space cloaking," *Opt. Lett*., vol. 38, pp. 1606-1608, 2013.
[16] A. Håkansson, "Cloaking of objects from electromagnetic fields by inverse design of scattering optical elements," *Opt. Express*, vol. 15, no. 7, pp. 4328-4334, 2007.
[17] L. S. Kalantari and M. H. Bakr, "Cloaking exploiting anisotropic adjoint sensitivity analysis," *IEEE Antennas and Propag. Soc. Int. Symp. Digest.*, Vancouver, BC, pp. 61-62, 2015.
[18] L. S. Kalantari and M. H. Bakr, "Wideband cloaking of objects with arbitrary shape exploiting adjoint sensitivities," *IEEE Trans. Antennas. Propag.*, vol. 64, no. 5, pp. 1963-1968, 2016.

Laleh Seyyed-Kalantari received the B.Sc. and M.Sc. degree with honors in Electrical Engineering (Telecommunications) from Sadjad Institute of Higher Education, Mashhad, Iran, in 2006 and University of Sistan and Baluchestan, Zahedan, Iran in 2009, respectively. She is currently pursuing the Ph.D. degree in Electrical Engineering at McMaster University, Hamilton, ON, Canada. In 2011, she joined the Computational Electromagnetic Laboratory (CEML), McMaster University. Her research interests include numerical method in electromagnetics, optimization of microwave and photonic devices, genetic algorithm and soft computing, metamaterials and cloaking.

Seyyed-Kalantari is a recipient of the Ontario Graduate Scholarship (OGS) Award in 2013, OGS and Queen Elizabeth II Graduate Scholarship in Science and Technology Award in 2014, and Research in Motion Ontario Graduate Scholarship Award in 2015.

Mohamed H. Bakr received a B.Sc. degree in Electronics and Communications Engineering from Cairo University, Egypt in 1992 with distinction (honors). In June 1996, he received a Master's degree in Engineering Mathematics from Cairo University. He earned the Ph.D. degree in September 2000 from the Department of Electrical and Computer Engineering, McMaster University. In November 2000, he joined the Computational Electromagnetics Research Laboratory (CERL), University of Victoria, Victoria, Canada as an NSERC Post Doctoral Fellow. He is currently with the Department of Electrical and Computer Engineering, McMaster University.

Bakr received a Premier's Research Excellence Award (PREA) from the province of Ontario, Canada, in 2003. He was a recipient of an NSERC DAS Award in 2011 and a co-recipient of the 2014 Chrysler Innovation Award. His research areas of interest include optimization methods, computer-aided design and modeling of microwave circuits and photonic devices, neural network applications, smart analysis of high frequency structures, and design of electric motors and power circuits.